Forensic Science International: Synergy 7 (2023) 100442

Contents lists available at ScienceDirect

Forensic Science International: Synergy

journal homepage: www.sciencedirect.com/journal/forensic-science-international-synergy

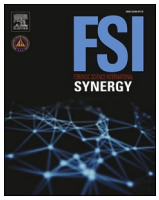

Forensic examination of a fragmentary funerary portrait in the collection of the Harvard art museums

Georgina Rayner [a,*], Katherine Eremin [a], Kate Smith [a], Caroline Cartwright [b], Patrick Degryse [c,d], Susanne Ebbinghaus [a]

[a] Harvard Art Museums, 32 Quincy Street, Cambridge, MA, 02138, United States
[b] British Museum, Department of Scientific Research, Great Russell Street, London, WC1B 3DG, United Kingdom
[c] KU Leuven, Earth and Environmental Sciences, Celestijnenlaan 200E, 3001, Leuven, Belgium
[d] Faculty of Archaeology, Leiden University, Einsteinweg 2, 2333CC, Leiden, the Netherlands

ARTICLE INFO

Keywords:
Roman Egypt
Composite
Technical imaging
Analysis
Workshop

ABSTRACT

The Harvard Art Museums' collection includes six Egyptian funerary portraits of the Roman period. These portraits are all that remains of the funerary equipment of individuals whose bodies were carefully prepared for burial and the afterlife. One example, depicting a man, is particularly complicated, broken into multiple fragments which have been glued down onto a board. The in-depth study of the portrait used a combination of non-invasive techniques, including X-radiography, infrared-, ultraviolet- and visible-induced luminescence imaging, and X-ray fluorescence spectroscopy to identify and locate particular pigments, binders and other artist materials, without needing to take a sample. Targeted sampling, informed by the imaging process, was then undertaken for additional analysis through the use of cross-sections, scanning electron microscopy with energy dispersive X-ray spectrometry, Fourier transform infrared spectroscopy, Raman spectroscopy, radiocarbon dating, and lead isotope ratio analysis. This study identified a core group of three fragments in the center of the portrait that comprise much of the face and neck, tunic, and part of the hair. The remaining 15 fragments contain most of the background, parts of the hair, and the proper left eye and tunic, and are distinct from the central group of fragments. Analysis suggests these fragments were reused from other ancient funerary portraits, and whilst it was not possible to connect any of these added fragments to one another, a potential workshop connection between the central fragments and three added fragments can be suggested based on a study of the composition of the lead white pigment, and similarities in painting technique.

1. Introduction

The collection of the Harvard Art Museums includes six funerary portraits from Roman Egypt. The portraits, five painted wooden panels (1923.56 and .60, 1924.80, 1939.111, 1946.44) and one three-dimensional plaster sculpture (1965.551), portray people who lived during the first three centuries CE, a time when Egypt was a province of the Roman empire. During this time the Egyptian tradition of preserving the body through the mummification process continued, but the funerary practice evolved to include portraits painted or sculpted in a more realistic manner. These portraits, placed over the face and, in the case of the wooden panels, incorporated into the wrappings of the mummified individuals they depict, highlight the multicultural nature of Egypt under Roman rule. Whilst their burials follow traditional Egyptian customs, the individuals represented in the portraits are shown in Graeco-Roman style, wearing clothing, hairstyles and jewelry that were popular in Rome.

The portraits in the collection of the Harvard Art Museums, like many others in collections around the world, have become dissociated from their original burial context and the bodies to which they belonged, unfortunately a common practice in the 19th and early 20th centuries. These portraits are all that remains of the funerary equipment of the individuals they represent, whose remains were carefully prepared for burial and the afterlife. Having their burials disinterred and dismantled some two thousand years later and the fragments distributed among modern collections is not what the deceased and their relatives would have hoped for. For the examples at Harvard, there are no records of the names of the deceased, their family members, or the artists; the burial

* Corresponding author.
E-mail address: georgina_rayner@harvard.edu (G. Rayner).

https://doi.org/10.1016/j.fsisyn.2023.100442
Received 8 May 2023; Received in revised form 26 September 2023; Accepted 9 October 2023
Available online 10 October 2023

Fig. 1. Composite portrait of a man, Egypt, early 2nd century CE. 29.3 × 13.2 cm. Harvard Art Museums/Straus Center for Conservation and Technical studies, Gift of Dr. Denman W. Ross.

sites are no longer known, and the archaeological context is lost because the excavation of the portraits was not documented. Learning about the portraits as material objects is one avenue available to us to remember the dead, thereby honoring the original intention of these works.

To this effect, the funerary portraits have been the subject of a multi-year intensive technical examination in the greater framework of the J. Paul Getty Museums' Ancient Panel Painting: Examination, Analysis, and Research (APPEAR) project [1]. The project, initiated in 2013, is a worldwide, multi-institution collaboration intended to develop a broader understanding of the methods, materials and workshop practices used to create these portraits. The research carried out in the Harvard Art Museums' Straus Center for Conservation and Technical Studies informed the recent exhibition *Funerary Portraits from Roman Egypt: Facing Forward* (August 26–December 30, 2022) [2].

Research conducted by participating institutions in the APPEAR project thus far has mostly focused on portraits painted on wooden panels, although examples on linen and three-dimensional masks are also known but not as widely researched. In the known corpus of portraits, there are rare examples where the portrait remains attached to the body [3]. The majority of portraits exist as separated but intact, or mostly intact panels or fragments of panels with varying degrees of damage. The portraits are typically painted in either encaustic, a technique which utilizes molten beeswax as the binder for the pigments, or tempera, which utilizes a proteinaceous medium such as animal glue or egg, or possibly a plant gum [4].

Published studies have focused on different aspects of the portrait manufacture, ranging from the general identification of materials which includes the identification and mapping of pigments non-invasively (for recent examples see Refs. [5–7]), or the characterization of organic materials, such as the use of whole egg as a coating applied on a portrait once it has been incorporated into the wrappings [8].

Historically, variation in portrait shape, for example rounded or angled corners, have been used to suggest a location of origin, and stylistic elements, such as jewelry and hairstyles, are used to date the portraits. Archaeological evidence, when it exists, may also be used (alongside analysis) to suggest a workshop connection [9,10]. By bringing many portraits together in one project, similarities in appearance are also being used to suggest a workshop connection. An example of this is the Saint Louis painter, named after the Portrait of a Woman [11] in the St Louis Art Museum collection. A recent multi-analytical study into portraits attributed to the St Louis painter [12] identified both similarities and differences in painting technique as well as variation in the materials used between multiple portraits. The authors concluded that these observations may indicate multiple painters, perhaps over multiple generations, working towards a common template in a workshop setting.

In a sense, all funerary portraits are fragments of a complete burial. Three of the portraits at Harvard are fragmentary themselves, broken from their original form to varying degrees. One of the more unusual fragmentary portraits is the composite portrait of a man (1924.80) (Fig. 1). This portrait arrived in the collection of what was then the Fogg Museum in 1924 as a gift from Harvard alumnus Denman Waldo Ross (1853–1935). Ross was a collector and painter, and taught design at Harvard and the Museum of Fine Arts in Boston. To facilitate research in this field, he built a "Study Series" at Harvard, comprising artworks as well as photographs, reproductions, and books – and included this and two other funerary portraits. Ross travelled widely, including Egypt. However, it is more likely that he acquired this portrait from a dealer in Europe or in New York City. This was a period when the trade in Egyptian antiquities flourished [13]. The Harvard Art Museums are actively engaged in researching the provenance of objects in the museums' collection, including the ancient Egypt funerary portraits, and are committed to making provenance information available in the museums' database and online collections (Guidelines to Collecting and Provenance, as well as to potential claims can be accessed via the museums' webpage [14]).

The portrait under investigation here is painted in encaustic. It depicts a young man with a nascent beard wearing a white tunic decorated with a dark blue or black *clavus* (stripe) or remnants of a cloak at the proper right side. In his dark black hair are the remnants of a wreath of gold leaves with a central flower. A red band studded with gold-colored buttons runs diagonally across his chest. This has been interpreted as a sword-belt. Men portrayed with these attributes are thought to have been members of the military, or perhaps officials of high rank who carried a sword [15]. Two such soldier portraits in the Antikensammlung in Berlin (31,161, 2; 31,161, 6) depict men with a short beard wearing a gold wreath [16]. Stylistically, these portraits are quite similar to the one at Harvard, and all three have been dated to the earlier 2nd century CE, during the reigns of the Roman emperors Trajan

Fig. 2. The composite portrait of a man labelled with the 18 separate fragments which make up the complete portrait.

(98–117) and Hadrian (117–138) [17,18]. The portrait at Harvard remains in the condition in which it was received by the museum in 1924: composed of 18 fragments (Fig. 2) glued down onto a tan-colored board.

As will be described in section 3, some of the fragments, especially at the left and right sides of the panel, appear mismatched. It is unknown when the portrait was assembled like this. In an early publication of the portrait, it was suggested that some of the fragments "may have been inserted during the period when the mummy stood in the house, where it might have become damaged, but we believe this portrait has also received modern doctoring" [19]. Most likely, the original portrait decayed during the almost two millennia of burial and was damaged when lifted from the mummified body, ending up in a fragmentary state. There are a small number of similar portraits, identified as composed of multiple fragments from several portraits [17,20–22], and it is widely accepted that these 'patchwork' portraits were created by antiquities dealers in Egypt, catering to collectors who wanted 'complete' objects [23]. Similar composites can be found among the late Roman, Byzantine, and early Islamic textiles, also from Egyptian tombs, that entered the market in the same period as the funerary portraits, namely the late 19th and early 20th centuries.

This paper describes the multi-analytical technical investigation of the composite portrait in Harvard's collection, framed as a forensic examination. In order to better understand the life of the portrait, the multiple fragments were studied to understand the materials and methods used to create them, with the goal of determining which of the multiple fragments may relate to one another. Multi-analytical projects to study an object in a museum collection are common in cultural heritage labs and overlap in many ways to the forensic examination of a crime scene. Both fields follow a similar approach, using close visual observation, followed by non-invasive technical imaging and scientific analysis to gather evidence which can then be interpreted through careful reasoning to establish a body of proof to support the resulting conclusions. It is worth noting, however, that differences also exist between the approaches used by the two fields. Namely, forensic examination is held to strict protocols/methodology and industry standards. It is difficult for cultural heritage scientists to adhere to such standards and the field lacks its own standard methodology because depending on the lab, not all examination techniques may be available and access to physical material in the form of samples for analysis is usually, if not always, limited. As such, gaps may exist when collecting evidence, so a different level of 'proof' exists when evaluating the history, condition or even authenticity of an object.

2. Materials and methods

2.1. Technical imaging

2.1.1. X-radiography (radiograph)

Computed X-radiography was carried out with a Comet MXR-320/26 tube and Carestream Industrex Flex HR detector plate.

The technical imaging described below was carried out with a Canon Mark III 5D DSLR camera and Zeiss 50 mm Makro-Planar ZE lens. The internal camera filtration was removed to allow for full bandwidth response at the detector. External filters and light sources were modified as described below:

2.1.2. Ultraviolet-induced visible fluorescence (UV) photography

PECA 918 and Wratten 2E filters and UV Systems Triple Bright 3 lights.

2.1.3. Visible-induced infrared luminescence (VIL) photography

Tiffen 87A filter and Sylvania LED 13 PAR 30LN bulbs.

2.1.4. Infrared digital photography (IRDP)

Tiffen 87A filter with Lowell Pro tungsten lights.

2.2. X-ray fluorescence spectrometry (XRF)

The XRF system employed is a Bruker Artax XRF spectrometer with a Silicon Drift Detector (SDD) and a rhodium anode X-ray tube. The primary X-ray beam is collimated to give a spot size of 0.65 mm. Using the Bruker Artax (version 7.6) software, spectra were acquired for 100 s live time at 50 kV and 600 μA. The dead time was around 2 %. Analysis was undertaken without a helium flux, resulting in poor detection of light elements (atomic number of potassium and lower).

2.3. Cross-section preparation

Samples for cross-section analysis were embedded in Bio-Plastic liquid polyester casting resin (Ward's Natural Science). Mounted

samples were ground to exposure using a Buehler Handimet 2 roll grinder with Carbimet abrasive paper rolls ranging in grit from 240 to 600. Samples were then polished using a Buehler Metaserv 2000 polisher with 6 μm and 1 μm Buehler MetaDi Monocrystalline Diamond Suspension.

2.4. Optical microscopy

Cross-sections were observed using a Zeiss Axio Imager.M2m upright microscope equipped with four objectives (5x, 10x, 20x and 50x) and a Zeiss Axiocam 512 Color digital camera. Images were captured using the Zeiss Zen 2.6 (blue edition) software. Visible light and bright field conditions utilized a halogen lamp and either an EPI-polarization filter cube or an EPI-Bright Field cube respectively. Ultraviolet (UV) conditions utilized a mercury vapor lamp and either a DAPI filter cube (excitation BP 450–490, beam splitter FT 510 and emission BP 515–565) or a FITC filter cube (excitation BP 450–490, beam splitter FT 510 and emission LP515).

2.5. Scanning electron microscopy with energy dispersive-ray spectrometry (SEM-EDX) of cross-sections

The cross-sections were analyzed using a JEOL JSM-IT500LV SEM (tungsten filament) with an Oxford Instruments X-MaxN SDD, 80mm2 detector (resolution Mn Kα, 126eV) running the Oxford Instruments AZtec software (version 4.2 SP1). The SEM was operated in low vacuum mode at a chamber pressure of 70Pa, with an operating voltage of 20 kV, beam current optimized for dead time below 10 % and working distance of 10 mm. The cross-sections were not coated prior to analysis.

2.6. Fourier transform infrared spectroscopy (FTIR)

FTIR in transmission mode was performed using a Bruker Vertex 70 infrared bench spectrometer coupled to a Bruker Hyperion 3000 infrared microscope. Samples were compressed on to a diamond cell with a stainless-steel roller prior to analysis. Using the Bruker OPUS (version 6.0) software, spectra were recorded between 4000 and 600 cm^{-1} at 4 cm^{-1} spectral resolution and 32 scans per spectrum. The collected spectra were compared to in-house and IRUG databases [24].

2.7. Raman spectroscopy

Raman analysis was conducted using a Bruker Optics Senterra dispersive Raman microscope with an Olympus BX51M microscope equipped with 20x and 50x long working distance objectives and using the Bruker OPUS (version 7.5) software. The Raman spectrometer has three laser sources, 532 nm, 633 nm and 785 nm. The optimum laser source depends on the pigment analyzed but in general, blue and green pigments were predominantly analyzed with the 532 nm laser at 2 mW or 5 mW power and other colors analyzed with the 785 nm laser at 10 mW power. Spectra were compared with reference libraries, particularly the RRUFF™ database [25], using the Opus software.

2.8. Wood identification

The following procedures were carried out in the laboratory of the Department of Scientific Research at the British Museum. Because of the three-dimensional nature of wood anatomy, each wood sample, irrespective of its size, was fractured manually to show transverse, radial longitudinal and tangential longitudinal sections (TS, RLS and TLS). Each TS, RLS and TLS wood section was then mounted onto aluminium stubs. Examination of the wood samples and comparative reference specimens (prepared and mounted using the same method) was undertaken in a variable pressure scanning electron microscope (VP SEM), Hitachi S–3700N, using the backscattered electron (BSE) detector at 15 kV, with the SEM chamber partially evacuated (40Pa). Magnifications ranged from ×35 to ×1000. The preferred working distance was c.14 mm but was raised or lowered from 10.6 mm to 16.5 mm (as required). With the BSE detector, 3D mode (rather than Compositional) was preferentially selected for maximum topographical information, and to maximize the potential for revealing diagnostic features for identification. Further details on wood identification methods and techniques can be found in Cartwright, 2015 [26] and 2020 [27].

2.9. Radiocarbon (^{14}C) dating

The Radiocarbon (^{14}C) dating service offered by the Center for Applied Isotope Studies at the University of Georgia [28] was used for dating of two wood samples taken from the portrait. The calibrated age ranges were obtained using the online OxCal v.4.4.4 software [29] using the IntCal20 calibration curve [30].

2.10. Lead isotope

Samples from 13 fragments had sufficient weight for Pb isotopic analysis. Of these, 3 (taken from fragments 9, 10 and 12) were composite samples, comprising samples taken from multiple locations on the same fragment to obtain enough material. The methodology was adapted from Rademakers et al. [31], dissolving the powdered sampled in strong acids and concentrating only the Pb fraction through ion exchange chromatography for multi collector–inductively coupled plasma–mass spectrometry (MC-ICP-MS) isotopic analysis.

3. Results and discussion

Analysis of the composite portrait of a man began with close visual examination, followed by non-invasive methods: a suite of non-invasive technical imaging consisting of ultraviolet induced fluorescence (UV) imaging, visible induced infrared luminescence (VIL) imaging, infrared photography (IRDP), X-radiography (radiograph), and X-ray fluorescence (XRF) spectroscopy. This was followed by secondary analysis using scientific methods to complement and/or confirm observations. This required selective sampling from the object. Samples were either mounted as cross-sections or left unmounted for analysis by a mixture of techniques, comprising scanning electron microscopy with energy dispersive X-ray spectrometry (SEM-EDX), Fourier transform infrared spectroscopy (FTIR), Raman spectroscopy, wood identification, radiocarbon dating, and lead isotope analysis.

3.1. Visual examination

The first step of the investigation focused on close looking, evaluating the portrait as a whole and then the individual fragments. This allowed initial observations and interpretations to be made.

Visual examination of the portrait reveals some fragments which do not fit well with the portrait as a whole. Fragments 8, 9 and 10, at the center of the portrait (Fig. 2), show most clearly the figure depicted. These three central fragments are well aligned and visually relate to one another. Conversely, fragments 1, 4 and 18, located towards the far left and right edges of the portrait and painted only with the light gray background, cause the body of the figure to stop abruptly when more of the figure's shoulders, including the remains of a military cloak, would be expected. Fragments 1 and 18, located on the far left and right edges of the portrait respectively, have areas left unpainted. It is likely that these two fragments belong to a portrait that had an unpainted area at the bottom of the panel, as can be observed in other portraits. The portrait of a gray-haired, bearded man in the Harvard Art Museums' collection (1923.59) [32], for example, includes an unpainted area at the bottom of the portrait that would have been covered by the wrappings when the portrait was attached to the mummified body. In their current condition there is no indication that the central fragments (8, 9 and 10) had an unpainted area that extended below the existing image.

Fig. 3. Detail showing the presence of a dark gray ground layer underneath the paint layer of the white tunic on the central fragments.

The lower edges of all the fragments at the bottom (and the upper edges of those at the top) of the portrait have been cut since they were painted. There is no evidence for the presence of wax or resin overlapping the edges of the portrait as might be expected if the edges were original. If an unpainted area was originally present, it was likely removed when the portrait was constructed into its current configuration.

Fragments, 7, 12–15, share elements with the portrait as a whole, but appear either slightly misaligned to the central figure, or misplaced entirely. This could have occurred when the portrait was reconstructed, leaving these fragments out of their original alignment. Fragment 7, a small rectangular fragment incorporated into the hair of the figure on the left-hand side, contains traces of the wreath of gold leaves similar to that present on the central fragments. Fragments 12–15 have been used to create a strip running the length of the portrait which completes the figure's face on the right-hand side, just off center from the central fragments in the current configuration. Fragment 12 incorporates the hair and golden wreath, fragment 13 the forehead and eyebrow, fragment 14 the remainder of the proper left eye and cheek, and fragment 15 the neck and white tunic.

Other fragments called into question include 2, 3 and 16. Fragments 2 and 3 are thin rectangular strips used to complete the figures face and hair on the left-hand side of the portrait. The hair in fragment 2 is painted differently to the rest of the portrait, with looser brush strokes and a touch of gray not seen in other fragments with hair. Fragment 3 has a significant amount of intact gilding in the background that does not match the rest of the portrait, which only has small remnants of gilding in the background close to the figure, visible on central fragment 8. The paint layer of fragment 16, a long, wide fragment on the far right-hand side of the portrait, is worn, resulting in a loss of the detail still present in the other fragments. Fragment 16 incorporates an ear and eyebrow and fits well to the face of the figure; however, the top edge of the hair is significantly higher than on all other fragments which include hair, and no gilded wreath is present.

The use of a dark gray ground layer can be seen under the surface paint layers of the central fragments 8, 9 and 10. It is most easily visible in areas of damage on the white tunic (Fig. 3). The same dark ground layer can be seen in areas of damage in the white tunic on fragment 15 to the right of the central fragments, as well as fragments 6, 11 and 12, which may suggest they relate to the main portrait preserved on the three central fragments (8, 9 and 10). Fragment 6 is a small square-ish fragment at the top of the portrait, painted only with the light gray background. Fragment 11, is a thin fragment with angled ends placed just off center to the right, which like fragment 12, incorporates the hair and golden wreath. No such ground layer appears to be present on the other fragments, suggesting they are unrelated to the central fragments (8, 9 and 10) and fragments 6, 11, 12 and 15.

Overall, the initial visual examination of the portrait identified that the three fragments (8, 9 and 10) at the center of the portrait are likely related. There are fragments in the wrong position, in particular, those at the far left- and right-hand edges, which cause the body of the figure to abruptly stop. It could be concluded from this that there may be pieces of

Fig. 4. Non-invasive technical images; a) X-radiograph (radiograhh), b) ultraviolet induced fluorescence (UV) image, c) visible induced luminescence (VIL) image and d) infrared digital photograph (IRDP).

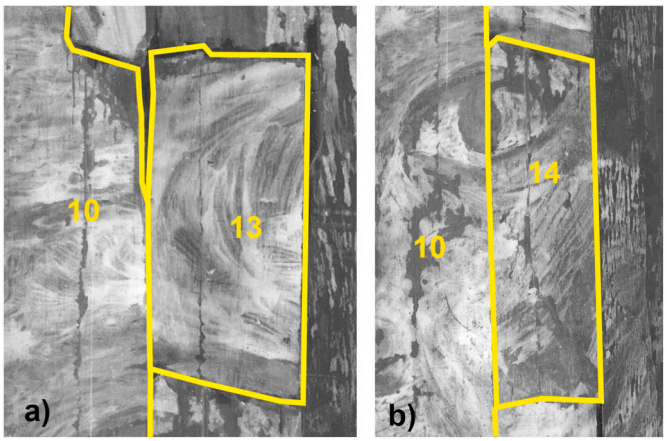

Fig. 5. Details from the radiograph of fragments 13 (a) and 14 (b), showing the different paint directions applied on the fragments compared to fragment 10.

the original portrait missing. Ultimately, it was observed that a large number of the fragments appear to have been painted differently, lacking the dark gray ground layer used on the central fragments. For those that do have the dark gray ground layer, they appear to be slightly offset from their original position.

3.2. Non-invasive analysis methods

The use of non-invasive technical imaging was used in the second step of the investigation. The techniques used here, X-radiography (radiograph), ultraviolet induced fluorescence (UV), imaging, visible induced infrared luminescence (VIL) imaging, infrared photography (IRDP), and X-ray fluorescence (XRF) spectroscopy, offer alternative views of the object being studied.

3.2.1. X-radiography (radiograph)

The radiograph of the portrait (Fig. 4a) reveals the brushwork because of the use of a high-density pigment such as lead white, basic lead carbonate ($2PbCO_3.Pb(OH)_2$), in the flesh tones, garment, and background in all fragments. In general, short paint strokes were used for the central fragments (8, 9 and 10), whilst longer sweeping strokes, often in differing directions, were used in the other fragments.

Examples of differences in paint application can be seen in fragments 13 and 14, two small rectangular fragments added to the right-hand side of the portrait to complete the figure's proper left eyebrow and eye. In fragment 13 the paint was applied in a circular motion that does not correlate with the paint application used for the rest of the figure's face (Fig. 5a), and therefore could not have been painted at the same time, assuming the portrait was intact when painted. On fragment 14 (Fig. 5b) the paint is also applied in a different direction to the rest of the figure's face. The difference is more subtle but is illustrated particularly well in the eye. In central fragment 10 the paint is applied to the white of the eye horizontally, but in the adjacent fragment 14 paint was applied vertically.

The radiograph provides further evidence that several fragments - fragments 1–4 on the left-hand side of the portrait, the small fragment 11 just off center to the right at the top, and the large fragment 16 on the right-hand side - are painted differently, as suggested either from visible examination (section 3.1) or from UV imaging (section 3.2.2). Fragments 6, 7, 12 and 15, fragments which surround the three central fragments incorporating the light gray background, hair, skin and tunic, could be related to the central fragments based on their relative densities and lines of paint application but are likely misplaced from their original alignment.

Fig. 6. Detail from the VIL image showing the presence of particles of Egyptian blue, visible as bright white specks, in fragments 1 and 16.

3.2.2. Ultraviolet-induced visible fluorescence (UV)

The glue used to adhere the fragments to the backing board fluoresces a pale blue color in the UV image (Fig. 4b), characteristic of an animal glue, and was confirmed as a proteinaceous medium by FTIR (Figure SI1). The adhesive can be seen in the cracks between the fragments and in larger splotches around the four main edges of the portrait. Past conservation treatments are also visible in the UV image, appearing as bright, incomplete strokes of added material on the surface, for example across the bridge of the man's nose.

The UV image also revealed areas of the light gray background, fragments 1 (painted only with the light gray background and running along the length of the left-hand edge), 4 (light gray background cutting of the shoulder of the figure on the left-hand side), 11 (in the hair just off center to the right), 16 (the long and wide fragment on the right-hand edge) and 18 (partially unpainted in the bottom right-hand corner), which fluoresced more brightly than the central fragments (8, 9 and 10). This variation in fluorescence suggests that the paint composition may be different in these fragments, indicating that they are not related to the central fragments.

No other characteristic fluorescence was noted, most significantly there was no evidence of madder lake. Made from the dye extracted from the roots of *Rubia tinctorum* and chemically bound to an inorganic material, such as alum (aluminum sulfate salts), madder lake fluoresces bright orange in UV and is often present in the flesh tones of Egyptian funerary portraits [33].

3.2.3. Visible induced infrared luminescence (VIL)

There are only a handful of pigments that can be visualized with VIL imaging; of these, of particular interest for Egyptian artifacts is Egyptian blue, a calcium copper silicate ($CaCuSi_4O_{10}$), widely regarded as the first man-made pigment [34,35].

Blue passages in the known funerary portraits are relatively rare [36]. The use of VIL to study funerary portraits has revealed that, despite the lack of blue color fields, Egyptian blue has been used more extensively than anticipated. Imaging shows Egyptian blue incorporated into pigment mixtures used to paint the skin-tones of figures, gray backgrounds and tunics (for examples see Refs. [5,36,37], perhaps added as an optical brightener [37].

There are no passages of blue in the portrait other than the dark blue or black band on the garment. The lack of response in the VIL image shows that this band does not contain Egyptian blue (Fig. 4c). However, the VIL image reveals the use of Egyptian blue in the majority of the fragments which make up the portrait, visible as bright white spots in the image (Fig. 6) and confirmed by selective sampling and FTIR analysis (Figure SI2).

Confirming the presence of Egyptian blue is significant because whilst it was used for centuries, the technology was considered lost by the 6th century CE [34]. Experiments began to characterize the pigment and reconstruct its synthesis in the 19th century, with a reproducible method found in the 1980s [35]. The portrait arrived in the Harvard Art Museums' collection in 1924, before Egyptian Blue was rediscovered. This indicates that the fragments which incorporate Egyptian blue in the

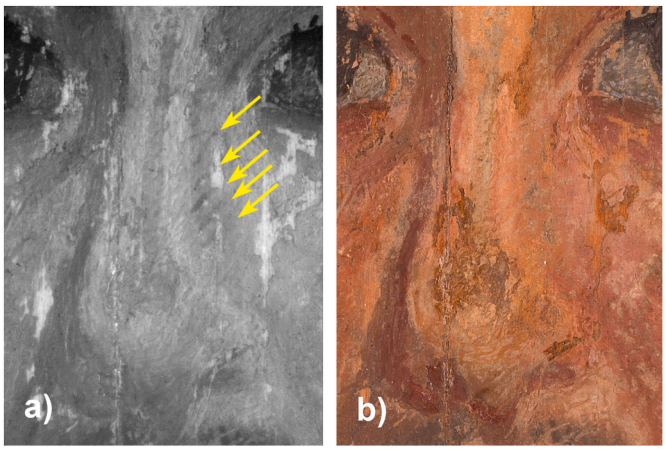

Fig. 7. Detail from the IRDP showing the observed underdrawing, highlighted by the yellow arrows, compared with the visible image (b) that shows these marks are not part of the surface paint layer.

paint layer are themselves ancient, likely from other damaged portraits.

The pigment has been used sparingly in the face (flesh-tones) of the figure, with only a faint scattering of particles observed, and no particles occur in the background gray color in the central fragments 8, 9 and 10. Conversely, Egyptian blue particles are concentrated in areas of the light gray background on both sides of the figure in fragments 1, 4 (to the left), 16 and 18 (to the right), already considered to be likely replacement fragments.

3.2.4. Infrared digital photography (IRDP)

Pigments such as lead white are transparent to infra-red, whilst others such as carbon black absorb IR and hence appear dark. This technique is therefore commonly applied to artworks to look through the surface layers and image preparatory sketches or underdrawings used by the artist to plan a composition.

These sketches are intended to be hidden by the final composition. Whilst not widely reported [38], the use of such sketches are known within the studied funerary portraits. A notable example resides in the collection of the Phoebe A. Hearst Museum of Anthropology at the University of Berkley, California. On the verso of a nearly erased portrait, a complete sketch of a female figure is present with instructions, written in Greek, for completing the portrait [39]. This example and others (for example see Ref. [40]) use a carbon-based pigment for the underdrawing, but other portraits have used gypsum (calcium sulfate, $CaSO_4$) [9] and Egyptian blue [37,41].

In the IRDP (Fig. 4d) of the portrait, evidence to suggest the use of preparatory drawing was apparent in central fragment 10. Here, five small dashes indicating a shadow on the proper left side of the nose are visible (Fig. 7a). These dashes are not replicated in the upper paint layer (Fig. 7b), indicating that these marks were made before the top layer of flesh-toned paint was applied. No other marks, or a more complete outline, were visible in the other associated central fragments (8 and 9), so it is not possible to know how extensive the preparatory sketch for the portrait was. There is no evidence for the use of a preparatory drawing or marks in any of the other fragments to the left or the right of the central ones.

3.2.5. X-ray fluorescence (XRF) spectrometry

XRF point analysis confirmed the use of a lead-rich pigment across the whole portrait, as indicated by the radiograph. The presence of lead can be attributed predominantly to the use of lead white, although in areas of the flesh and the red sword belt, the use of red and yellow lead-based pigments, such as minium (lead tetroxide, Pb_3O_4) or massicot (lead oxide, PbO), cannot be ruled out by this analysis. High levels of iron, corresponding to ocher pigments, such as hematite (iron oxide, Fe_2O_3) and goethite (iron hydroxide, FeO(OH)), are found throughout the portrait, particularly concentrated in the flesh tones and facial features of the man. Generally, the absence of evidence for other colorants in the cloak, light gray background and hair across all fragments suggest the use of a carbon black-based pigment alongside lead white and ocher to create these colors. The presence of bone black (calcium phosphate, $Ca_3(PO_4)_2$) cannot be ruled out from this analysis as phosphorus can be difficult to detect, particularly without the use of helium during analysis.

XRF point analysis targeting areas of brightest VIL response in the light gray background on fragments on either side of the figure, 1 and 4 (on the left) and 16 (on the right), and in the flesh tones of central fragment 9, showed elevated copper levels compared to the general background indicating the presence of Egyptian blue, confirmed with a sample and FTIR analysis. None of those spectra showed any tin which would suggest the use of bronze in the manufacture of the pigment [35].

Areas of gilding, a thin layer of metal applied to surfaces as a decorative finish, have high levels of gold with trace levels of silver and show no significant difference between the central fragments and those surrounding them. Iron, calcium and lead are all detected in these areas, and likely reflect the presence of lead white and ocher beneath the gilding (Figure SI3).

3.3. Summary

The use of technical imaging to study the portrait helped confirm some of the initial observations made about fragments during the visual examination that suggested they may not be related to the central fragments. The use of x-radiography identified fragments that had been painted with a different paint, observed to have a lower density in the radiograph, or painted in a different manner, evidenced by different directions of brushstrokes. With UV illumination fragments painted with a different paint, likely a different pigment to binder ratio, were observed. The use of VIL identified pigments which incorporated Egyptian blue into the paint, particularly in areas of the light gray background, which contrasts with areas of background on the central fragments.

Whilst the use of infrared reflectography and x-ray fluorescence did not help with determining which fragments relate to one another, the two techniques offered insight into the methods, such as selective underdrawing, and pigments used by the artist.

3.4. Invasive analysis methods

The final step of the investigation utilized invasive analytical methods to scientifically identify materials present to better understand the observations made using the non-invasive methods. To perform the analysis described throughout this section, a selection of small samples were taken from the portrait. Sampling is invasive; however, only minute amounts of material were removed and only from existing areas of damage along break lines to minimize disruption of the object's surface. Samples can be analyzed by more than one method, reducing the need for larger, or multiple samples to be taken. Samples were not taken from fragments that did not have suitable areas. For that reason, fragments 5 and 11, small rectangular fragments incorporated into the hair on either sides of the central fragments (8, 9 and 10), and fragment 17, a small unpainted triangular fragment embedded in fragment 16 on the far right-hand side of the portrait (Fig. 2), were not sampled.

Sampling aimed to capture all of the layers present, from the surface paint layer through to the wooden panel. In practice, the wooden panel was rarely captured and when it was, the sample often did not remain intact, cleaving at the interface of the panel with the paint or (where present) the dark gray ground. The majority of samples were prepared as cross-sections, allowing the paint stratigraphy and elemental composition to be studied in greater detail with optical microscopy and SEM-EDX. FTIR and Raman were also used to aid with pigment identification in the samples where possible.

Table 1
Results from the wood identification and radiocarbon measurements of the wood samples from fragment 15 and 18.

Fragment	Wood Identification	Radiocarbon dating		
		14C age, years BP	Calibrated age (68.3% probability)	Calibrated age (95.4% probability)
11	*Tilia europaea*	–	–	–
15	*Tilia europaea*	2050 ± 20	95 - 74 BCE (18.1 %) 56 - 34 BCE (26.4 %) 16 BCE - 6 CE (23.8 %)	148 - 138 BCE (1.6%) 110 BCE - 21 CE (93.8 %)
18	*Tilia europaea*	1870 ± 20	130 - 144 CE (13.3 %) 155 - 211 CE (54.9 %)	124 - 226 CE (95.4 %)

BCE: before common era, CE: common era.

3.4.1. Wooden support

Samples of wood were taken for identification of the wood species and radiocarbon dating to understand the wooden panel onto which the portrait(s) were painted. Whilst samples for wood identification can be small, approximately 1 mm × 1 mm, accessing the edges or verso of the fragments for sampling was hindered by the board to which they are adhered. As a result, samples could only be taken from fragments 11, a thin fragment with angled ends which incorporates the hair and golden wreath, 15, a longer fragment which completes the figures neck and tunic, and 18, a wider and mostly unpainted fragment, all on the right-hand side of the portrait. Fragments 15 and 18 had damage to their edges, whilst the back of fragment 11 was partially accessible. Samples for radiocarbon (^{14}C) dating are significantly larger than typical samples. Ultimately, only two samples could be taken from the portrait, from fragments 15 and 18. No wood samples could be taken from the three central fragments (8, 9 and 10) for wood species or radiocarbon dating.

The use of *Tilia europaea*, also known as lime or linden tree, was identified for all three samples [42]. The distinguishing features of *Tilia* species are fully described and illustrated in Ref. [27]. Lime is not native to Egypt, so was imported from Europe where it was widely available and is the most commonly encountered European wood identified in Egyptian funerary portraits [15]. Lime is well suited for manufacture of the boards for the portraits, unlike native Egyptian wood, such as Ficus sycomorus which is of poor quality, requires cutting into thicker planks and is prone to insect attack. A high-quality wood, lime cuts/carves well and can be bent to produce a curved panel [27]. It is not known how or why lime wood became the popular choice for funerary portraits in Egypt.

The results from the radiocarbon measurement are shown in Table 1. Based on the results, fragment 15 has an estimated age within the 2nd century BCE and the early 1st century CE, most likely between 110 BCE–21 CE. Fragment 18 has an estimated age within the 2nd and 3rd centuries CE, more specifically between 124 and 226 CE. This difference in age shows that fragments 15 and 18 could not be part of one original, intact, wooden panel. The date measured for fragment 15 is significantly older than the mid-2nd century date attributed to the portrait on stylistic grounds. However, since it was not possible to obtain wood samples from the three central fragments (8, 9 and 10), it is not possible to say whether the man was painted on older wood, which would be compatible with the dating of fragment 15 (although other features also suggest this fragment is separate). The older date of the wood suggests this fragment may come from an older portrait, or was painted on re-used wood. In contrast, although the wood of fragment 18 is roughly contemporaneous with the imagery of the portrait, this fragment has been shown on the basis of other criteria (presence of Egyptian blue, UV fluorescence and absence of a dark gray ground layer) to be distinct from the central fragments (8, 9 and 10).

The identification of two fragments with different but ancient ages shows that at least one, and probably more, fragments were taken from other ancient portraits, also shown by the presence of Egyptian blue in some painted areas. Whilst there is no documentary proof of this, it remains likely that multiple, unrelated fragments were added to the central fragments to make a 'complete' composition in the early 20th century prior to its sale in the antiquities market.

3.4.2. Dark gray ground layer

The dark gray ground that is present on the central fragments is illustrated in the cross-section prepared from a sample taken from fragment 9 (Fig. 8a). It contains fine black particles, best seen in the UV image (Fig. 8b), with large, often angular particles (varying in size from approximately 8 × 11μm up to 90 × 27μm) all surrounded by a matrix of finer pigment particles. Elemental mapping of the sample (Fig. 8c) shows that the large particles are calcium carbonate ($CaCO_3$), colored red in the map, and they are surrounded by finer particles of both calcium carbonate and calcium sulfate ($CaSO_4$). Analysis by FTIR identified the specific phases calcite and gypsum (Figure SI4). The gypsum appears orange in the map as it is a combination of calcium, colored in red, and sulfur, colored in yellow. A small amount of silicate phases, colored green, are also present.

The dark gray ground layer was captured in cross-section for fragments 6, the small square-ish fragment at the top to the left of the figure, painted only with the light gray background, fragment 12, a small rectangular fragment at the top which incorporates the hair and golden wreath, completing the figure's hair on the right-hand side and fragment 15, a longer fragment at the bottom which completes the figure's neck and tunic on the right-hand side. Analysis identified a similar mixture of calcium carbonate and calcium sulfate, as well as the likely presence of carbon black. However, the large angular particles of calcium carbonate observed in the ground of the central fragments were not present in these samples. A large angular particle (8 × 12μm) was present in the ground layer of fragment 12 (see Fig. 10d later) but was identified as a silicate instead of a carbonate. It should be noted that the ground layer in samples from fragments 6, 12 and 15 was never of comparable thickness to that in the sample from fragment 9 (60–80 μm for fragment 9 versus 16–23 μm for fragment 6, 10–25 μm for fragment 12 and approximately 15 μm for fragment 15). It is unlikely that the complete ground layer was captured during sampling as these samples did not contain the wooden panel in cross-section. Hence, although it appears that the larger particles of calcium carbonate are not present in the ground of fragments 6, 12 and 15, it cannot be ruled out that these would be observed if larger samples could be obtained.

3.4.3. Surface paint layer

A single paint layer was present in most cross-sections. Multiple layers were only observed for the blue/black coat and red sword belt, which were painted over the white tunic, and where areas of gilding were applied over the paint layer in the light gray background and hair.

A limited selection of pigments were identified in the samples analyzed. They were used consistently across all fragments and were typical of the Egyptian palette [43,44]. Analysis of the paint layers confirmed the use of lead white and red and yellow ochers throughout the portrait, with the lead white more concentrated in the tunic and the ochers more concentrated in the flesh tones. The light gray background in all fragments is a mixture of pigments; lead white, ocher and a carbon-based black. Raman spectroscopy identified the ochers as containing hematite and goethite (Figure SI5). In samples from some fragments, and as previously discussed in section 3.2.3, Egyptian blue was present. Natrojarosite, a sodium iron sulfate ($NaFe_3(SO_4)_2(OH)_6$), was additionally found scattered in varying amounts across the different fragments of the portrait (background, skin and tunic) (Figure SI6). The pigment in the blue/black cloak has not been conclusively identified. In cross-section it appears dark and lacks significant inorganic elements, indicating that it is organic-rich. No evidence was found for indigo using

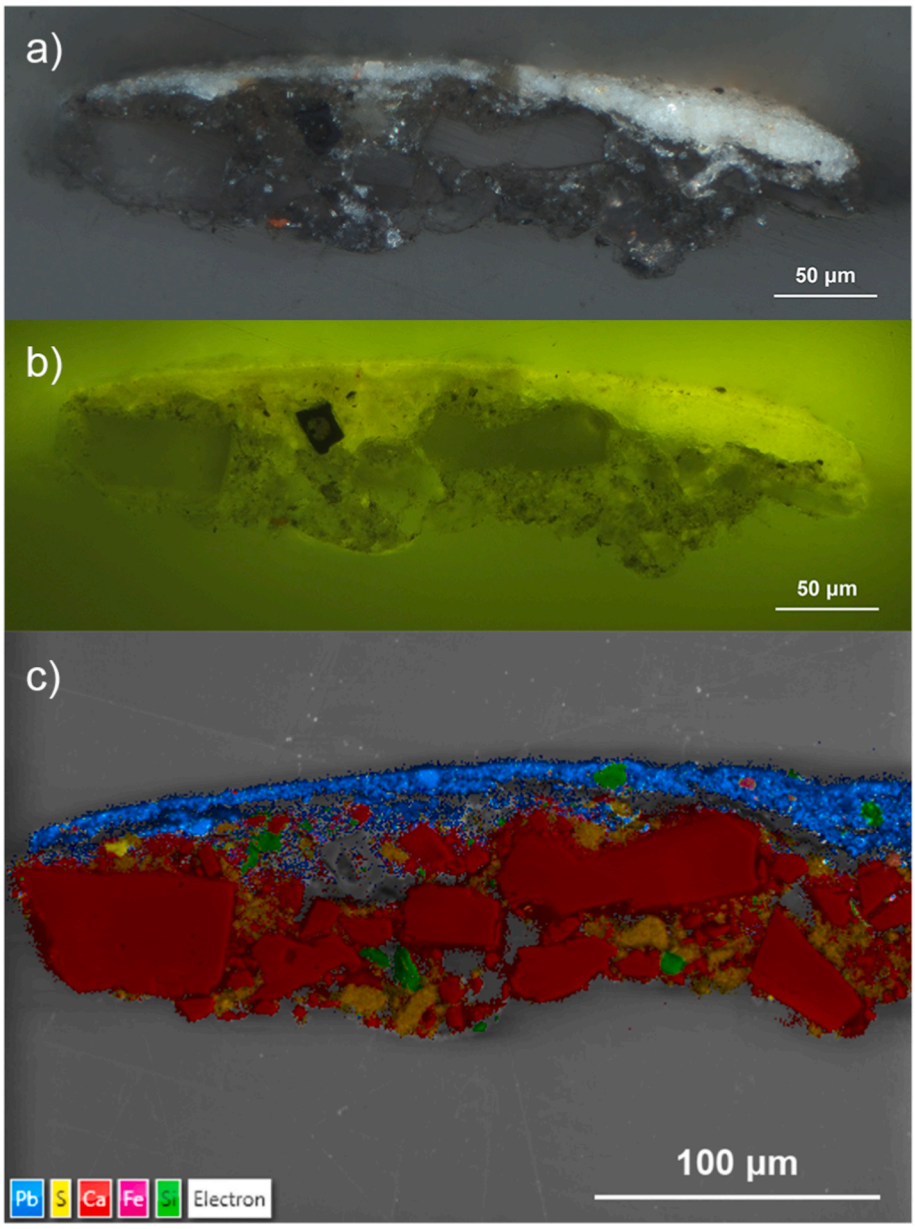

Fig. 8. Cross-section prepared from central fragment 9 in visible light (a), with ultraviolet irradiation (b) and the backscattered electron image overlaid with the elemental map (c) showing Pb in blue, S in yellow, Ca in red, Fe in pink and Si in green.

FTIR and Raman, so it is likely that a carbon-based black was used.

Cross-sections were particularly useful to investigate why the light gray background in fragments 1 (a fragment with only the light gray background, running along the length of the left-hand edge), 4 (a fragment of light gray background cutting of the shoulder of the figure on the left-hand side), 11 (a small fragment in the hair just off center to the right), and 18 (a partially unpainted fragment in the bottom right-hand corner) fluoresced differently with ultraviolet light compared to the three central fragments (8, 9 and 10). In Fig. 9 cross-sections prepared from the samples taken from fragment 1 and central fragment 10 are compared. Most strikingly, in the visible light image, the cross-section from central fragment 10 (Fig. 9a) appears more opaque and brighter white than the more translucent and off-white cross-section from fragment 1 (Fig. 9c), indicating a higher proportion of lead white to binder in fragment 10. This observation was confirmed in the back-scattered electron (BSE) images. In the sample taken from fragment 10 (Fig. 9b), the paint layer is densely packed with a mixture of fine and coarse particles of lead white (appearing bright white in the BSE image). Conversely, the sample from fragment 1 (Fig. 9d) has significantly less of these bright white particles distributed within a dark matrix, indicating a lower proportion of lead white within the organic binder. This indicates that the paint film has a higher organic content, in this case wax, and the bright fluorescence observed in the UV image is coming from this higher proportion of wax. The same low pigment concentration was seen for the other fragments which fluoresced (4, 11 and 18), and indicates that these fragments were not painted at the same time as the central fragments (8, 9 and 10).

A similar comparison was undertaken with fragments 6 and 12. Both fragments form part of the light gray background, with fragment 6 being the small square-ish fragment at the top of the portrait, just off center to the left, painted only with the light gray background, and fragment 12, being the small rectangular fragment at the top of the portrait which also incorporates the hair and golden wreath, completing the hair of the figure on the right-hand side, along with the light gray background. Throughout the study, neither fragment had been ruled out from being part of the central portrait. If this were to hold true, these fragments

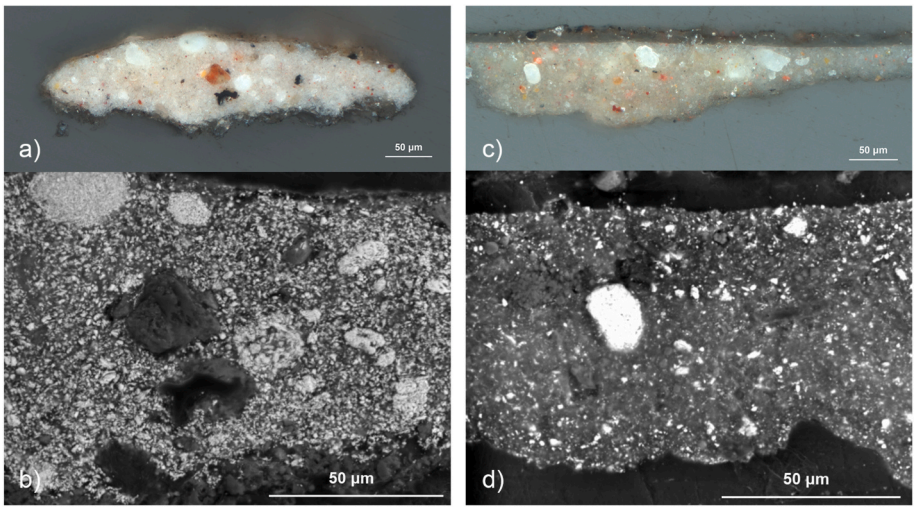

Fig. 9. Cross-sections prepared from areas of the light gray background on fragments 10 (left) and 1 (right) in visible light (top row) and the BSE images (bottom row) showing a detail of the cross-section illustrating the pigment distribution in the paint layer.

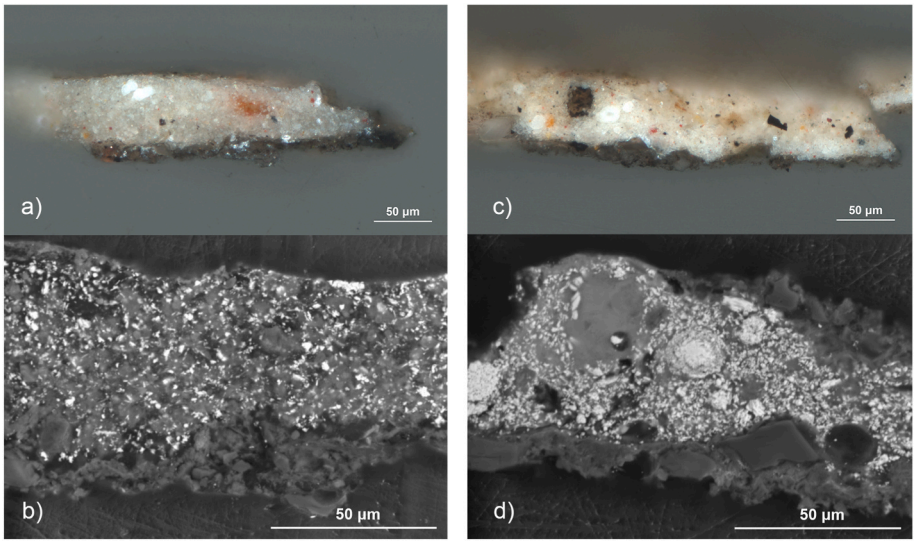

Fig. 10. Cross-sections prepared from areas of the light gray background on fragments 6 (left) and 12 (right) in visible light (top row) and the BSE images (bottom row) showing a detail of the cross-section illustrating the pigment distribution in the paint layer.

would be expected to have a comparable paint layer to that used in the background on the central fragments (Fig. 9a and b). The paint film in the cross-section prepared from fragment 6 (Fig. 10a and b), lacks the multiple, large lead white aggregates present in the paint layer from the central fragments. The finer particles of lead white also appear to be less densely packed. Overall, this suggests that a different paint was used for the paint layer in the background of fragment 6. The paint from fragment 12 (Fig. 10c and d) looks more similar to the paint in the central fragments but has an unusual "swirled" texture.

The observed difference in the pigment/binder ratio was not limited to the light gray background. It was also observed in cross-sections prepared from fragment 14 (a small rectangular fragment which incorporates the remainder of the proper left eye and cheek, on the right-hand side of the figure), already suggested by X-radiography to be a replacement piece, and fragment 15 (a longer fragment which incorporates the neck and white tunic, on the right-hand side of the figure). This was the first suggestion that fragment 15 was different from the central fragments. Until this point, fragment 15 was thought to be related to the central fragments but slightly misplaced in the current composition. The radiograph was particularly compelling as the painted brush strokes match directionally from the tunic in fragment 15 to those of the tunic in the central fragments 9 and 10. In addition, fragment 15 has the same dark gray ground layer as the central fragments.

The white paint layer used for the tunic on the central fragments and that used for fragment 15 are elementally similar. They contain lead white, a calcium-rich mineral (most likely calcite) and a scattering of natrojarosite. Visually, the paint films from the two fragments are very different. The white tunic on the central fragments is painted similarly to the corresponding light gray background. The paint layer is densely packed with a mixture of fine and coarse particles of lead white, as shown for fragment 9 (Fig. 11a and b). The paint film from fragment 15 (Fig. 11c and d) is very organic rich (appearing dark in the BSE). It has large aggregates of lead white (appearing bright white in the BSE) but does not have the same dense distribution of fine lead white particles that is seen consistently in samples of paint from the central fragments. This is a clear indication that the paint layer in fragment 15 could not have been applied using the same paint or brush strokes as those of fragments 9 and 10.

The lead isotopic composition (Pb IC) of the samples analyzed reflects the origin of the lead used for making the lead white pigment

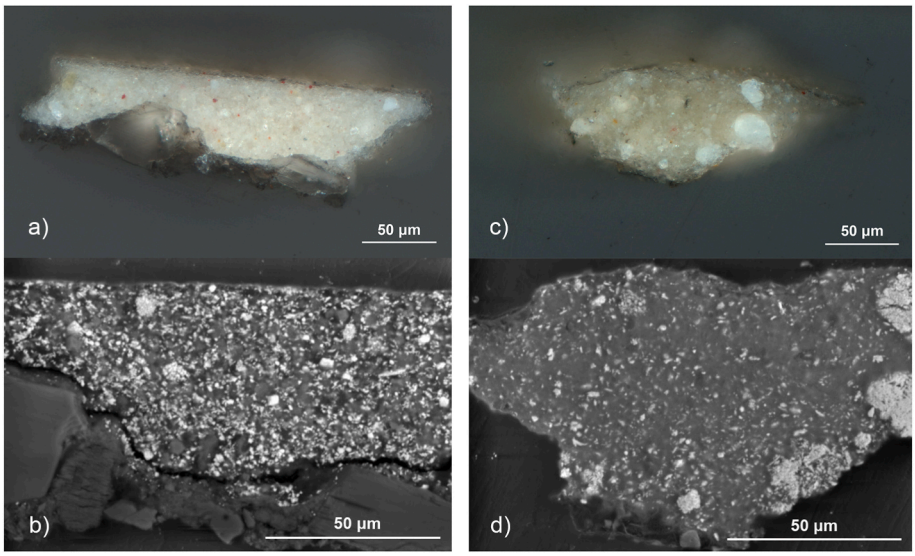

Fig. 11. Cross-sections prepared from areas of the white tunic on fragments 9 (left) and 15 (right) in visible light (top row) and the BSE images (bottom row) showing a detail of the cross-section illustrating the pigment distribution in the paint layer.

Table 2
Lead isotope ratios of the samples taken from the multiple fragments comprising the portrait.

Fragment	Area sampled	$^{206}Pb/^{204}Pb$	±2σ+	$^{207}Pb/^{204}Pb$	±2σ+	$^{208}Pb/^{204}Pb$	±2σ+
1	Light gray background	18.501	0.037	15.641	0.032	38.420	0.079
2	Hair	18.647	0.013	15.671	0.013	38.773	0.037
4	Light gray background	18.575	0.025	15.664	0.024	38.676	0.074
6	Background	18.321	0.021	15.643	0.020	38.451	0.055
8	Skin	18.304	0.008	15.604	0.007	38.388	0.016
	Light gray background	18.367	0.013	15.696	0.013	38.623	0.035
9	Composite sample (tunic and light gray background)	18.272	0.008	15.610	0.007	38.389	0.018
10	Composite sample (skin, hair and light gray background)	18.252	0.007	15.602	0.006	38.350	0.015
	Tunic	18.324	0.016	15.641	0.015	38.444	0.043
11	Light gray background	18.392	0.017	15.662	0.016	38.514	0.048
12	Composite sample (hair and light gray background)	18.308	0.005	15.614	0.005	38.409	0.012
13	Skin	18.375	0.006	15.575	0.005	38.313	0.013
15	Skin	18.362	0.017	15.678	0.016	38.574	0.059
	Tunic	18.348	0.024	15.675	0.022	38.553	0.114
16	Light gray background	18.636	0.007	15.622	0.006	38.637	0.014
	Skin	18.306	0.021	15.640	0.019	38.434	0.055
18	Light gray background	18.432	0.025	15.643	0.022	38.450	0.058

found within the paint used across the various fragments of the portrait. This analysis was undertaken to support the results from the technical investigation thus far, which determined that all fragments (with the exception of 17, the small unpainted triangular fragment embedded in fragment 16) other than the central fragments 8, 9 and 10 are likely not part of the original composition.

All $^{206}Pb/^{204}Pb$ values range between 18.252 and 18.647, the $^{207}Pb/^{204}Pb$ ratio ranges between 15.575 and 15.696, and the $^{208}Pb/^{204}Pb$ values range between 38.313 and 38.773 (Table 2) for the samples analyzed. In terms of range of Pb IC of all fragments, this appears to be consistent with the full range of Pb used in the Roman empire [45].

Central fragments 8 and 10, along with fragments 15 (a longer fragment in the bottom half of the portrait, just off center to the right, incorporating the neck and white tunic, on the right-hand side of the figure) and 16 (a long and wide fragment on the far right-hand side of the portrait with worn paint) each had two samples from different locations on the fragment analyzed. The Pb IC of fragment 15 is homogenous, illustrated in Fig. 12 with both data points in close proximity, indicating that the same source of lead was used for the two different areas (skin and tunic) sampled from the fragment. Fragments 8, 10 and 16 show a different Pb IC for the two samples analyzed. This inhomogeneity in Pb IC for these fragments might suggest the use of different batches of lead white to paint different areas on a single fragment. Contamination of the Pb IC of the lead white pigment by some other material in these samples, such as the presence of other pigments like Egyptian blue, could also cause such a discrepancy. However, this was deemed unlikely in view of the extremely high Pb content of lead white.

Intercomparing fragments, the central fragments 8 (one sample, skin), 9 (composite sample of tunic and light gray background) and 10 (both samples, tunic and composite of skin, hair and light gray background) along with 6 (light gray background), 12 (composite sample of hair and light gray background) and 16 (one sample, skin) show a narrow range in Pb IC, as do central fragment 8 (second sample, light gray background) and 15 (both samples, skin and tunic). Whether this is indicative of the use of a similar lead white and thus a common origin, is unclear. More broadly, it could be suggested that fragments 6, 8–10, 12 and 15 fall within a similar but wider range. These results open up the possibility that perhaps fragments 6, 12 and 15, whilst not to be related to the central fragments of the Harvard portrait (as determined by other analytical methods described previously), could be related to one another, coming from other portraits painted in the same workshop as the central fragments using the same batches of lead white pigment.

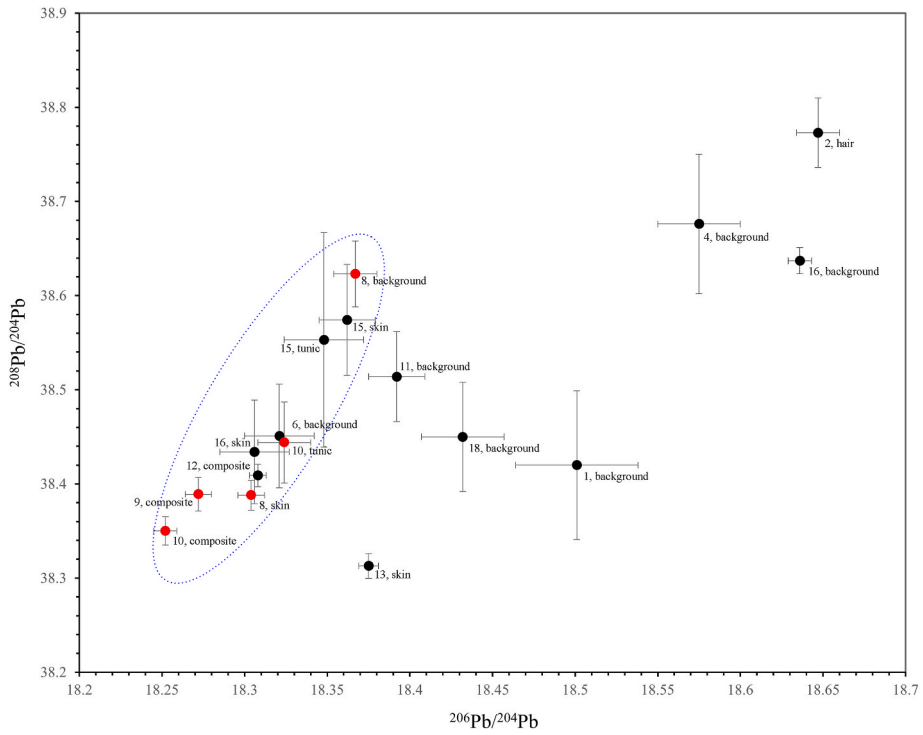

Fig. 12. Isotope ratio biplot showing the lead (Pb) isotope ratios of the samples taken from the multiple fragments comprising the portrait. Points colored red represent the central fragments 8, 9 and 10. Samples encircled by the blue dotted ellipsis (graphical representation only, no statistical value is meant) are taken from fragments that are thought to have used the same source of lead white pigment.

All other fragments from across the portrait that were analyzed (1, 2, 4, 11, 13, 16 [excluding the skin sample] and 18) have an Pb IC separate from the other fragments, likely confirming the use of other compositions of lead white, possibly indicative of a different origin or workshop, as suggested from the other analyses conducted.

3.5. Summary

The study of wood type and age identified the use of the same wood across three fragments; however, the dating implies that these are from different sources. Whilst not all fragments, including the central fragments, could be analyzed this way, this data helps corroborate the idea that not all fragments belong to this portrait.

Study of the dark gray ground layer was inconclusive as it was difficult to capture the full cross-section from top of paint layer to wood. However, in cross-section, differences in paint formulation were apparent for these same fragments, indicating a different paint was used for these and the central fragments. The same was true for fragments that fluoresced differently with UV illumination, where it was observed that a different pigment to binder ratio in comparison to the central fragments had been used. It is important to note that the use of cross-sections also confirmed the three central fragments were consistent with one another in terms of materials and painting method.

The final analysis undertaken was a study of lead isotopes. This suggests that some fragments may have used the same lead source for the paint, despite the fact that other analysis rules indicates these fragments are not original. This could indicate a possible workshop connection between the central fragments of the portrait and some of the added fragments.

4. Conclusions

A combination of close visual examination, non-invasive and invasive methods of analysis were used for the in-depth technical study, framed as a forensic examination, of the fragmentary funerary portrait in the Harvard Art Museums' collection. The initial use of close looking and non-invasive imaging provided a wealth of information that formed the initial identification of the three related fragments (8, 9 and 10) which depict the male figure, likely a soldier, at the center of the portrait, as well as irregularities in many of the surrounding fragments. The selective sampling which followed allowed for the identification of wood type and age, painting methods, and paint composition and stratigraphy across the fragments of the portrait.

The three central fragments are painted similarly, with a dark gray ground containing calcite and gypsum, and the paint composition is consistent-large aggregates of lead white are present and Egyptian blue is used sparingly and may be unintentional.

The other fragments, with the exception of fragment 17, which could not analyzed as it is a small, inaccessible piece of unpainted wood, were found to have multiple visual and material differences to the central fragments 8, 9, and 10. This study has shown differences in UV fluorescence for some fragments compared to the central fragments, attributed to a difference in pigment to binder ratio. It also revealed more extensive use of Egyptian blue than expected, different brushwork, painting methods and paint morphology for the majority of the fragments.

By comparing the results from multiple analyses, a body of evidence has been gathered for each fragment that can be used to determine whether or not that fragment originally belonged to the same portrait as the central fragments (Table 3). One fragment, fragment 16, 'failed' in every category of the investigation. The majority of the others failed as the investigation moved from macro to micro, from the use of imaging to the analysis of paint composition. The evidence gathered in this study is enough to determine that this is not a single portrait that has been broken into multiple fragments. It remains likely that the portrait was broken when removed from the burial site, and then reconstructed with other similar looking fragments, before it was sold on the art market. The fate of the other fragments that would have been part of the original composition is unknown.

The pigment palette, wood type and age, suggests that these added

Table 3
Summary of results which led to the identification of fragments unrelated to the central fragments 8, 9 and 10 using different techniques.

Fragment	Description	Visual examination		Non-invasive technical imaging			Invasive analysis (samples)		Overall determination
		Surface paint layer	Dark gray ground	Radiograph	UV	VIL	Paint composition	Pb isotope	
1	fragment running the length of the portrait on the left-hand edge, painted only with the light gray background	not enough information visible to make determination	absent	unrelated based relative density of paint	unrelated due to difference in fluorescence	unrelated due to use of Egyptian blue	more binder rich	different lead source	non-original
2	thin rectangular fragment on the left-hand side of the portrait, used to complete the figures hair and face	visibly unrelated	absent	unrelated based on brushstrokes	possibly unrelated due to slight difference in fluorescence	No response	different composition to central fragments	different lead source	non-original
3	thin rectangular fragment on the left-hand side of the portrait, used to complete the figures face	visibly unrelated	absent	unrelated based on brushstrokes	possibly unrelated due to slight difference in fluorescence	No response	different composition to central fragments	(not sampled)	non-original
4	a thin rectangular fragment, bottom half of the portrait on the left-hand side, painted only with the light gray background, cutting of the shoulder of the figure	not enough information visible to make determination	absent	unrelated based relative density of paint	unrelated due to difference in fluorescence	unrelated due to use of Egyptian blue	more binder rich	different lead source	non-original
5	very thin fragment, at the top of the portrait on the left-hand side, incorporated into the hair	possibly related but misaligned	absent	could be related	fluorescence matches central fragments	No response	(not sampled)	(not sampled)	non-original
6	small square-ish fragment at the top of the portrait, just off center to the left, painted only with the light gray background	possibly related but misaligned	present	could be related	fluorescence matches central fragments	No response	pigment morphology is different, more binder rich	possibly the same source of lead	non-original
7	small rectangular fragment incorporated into the hair, just off center to the left, traces of a wreath of gold leaves	possibly related but misaligned	absent	could be related	fluorescence matches central fragments	No response	different composition to central fragments	(not sampled)	non-original
8–10	central fragments	well aligned with cohesive imagery	present			trace response			original
11	thin fragment with angled ends, at the top of the portrait, just off center to the right, incorporates the hair and golden wreath	possibly related but misaligned	present	unrelated based relative density of paint	unrelated due to difference in fluorescence	No response	more binder rich	different lead source	non-original
12	small rectangular fragment at the top of the portrait, just off center to the right, incorporates the hair and golden wreath	possibly related but misaligned	present	could be related	fluorescence matches central fragments	No response	pigment morphology is different, more binder rich	possibly the same source of lead	non-original
13	small rectangular fragment, incorporates the forehead and eyebrow, on the right-hand side of the figure	possibly related but misaligned	absent	unrelated based on brushstrokes	possibly unrelated due to slight difference in fluorescence	No response	different composition to central fragments	different lead source	non-original
14	small rectangular fragment, incorporates the remainder of the proper left eye and cheek, on the right-hand side of the figure	possibly related but misaligned	absent	unrelated based on brushstrokes	possibly unrelated due to slight difference in fluorescence	No response	different composition to central fragments	(not analyzed)	non-original

(*continued on next page*)

Table 3 (*continued*)

Fragment	Description	Visual examination		Non-invasive technical imaging			Invasive analysis (samples)		Overall determination
		Surface paint layer	Dark gray ground	Radiograph	UV	VIL	Paint composition	Pb isotope	
15	longer fragment in the bottom half of the portrait, just off center to the right, incorporates the neck and white tunic	possibly related but misaligned	present	could be related	fluorescence matches central fragments	No response	different composition to central fragments	possibly the same source of lead	non-original
16	long and wide fragment on the far right-hand side of the portrait, worn paint	visibly unrelated	absent	unrelated based relative density of paint and brushstrokes	unrelated due to difference in fluorescence	unrelated due to use of Egyptian blue	different composition to central fragments	different lead source	non-original
17	small unpainted triangular fragment embedded in fragment 16	not enough information visible to make determination	absent	no paint present	(no observable fluorescence)	No response	(not sampled)	(not sampled)	could not be determined
18	Rectangular fragment, bottom right-hand corner, partially unpainted	not enough information visible to make determination	absent	unrelated based relative density of paint	unrelated due to difference in fluorescence	unrelated due to use of Egyptian blue	more binder rich	different lead source	non-original

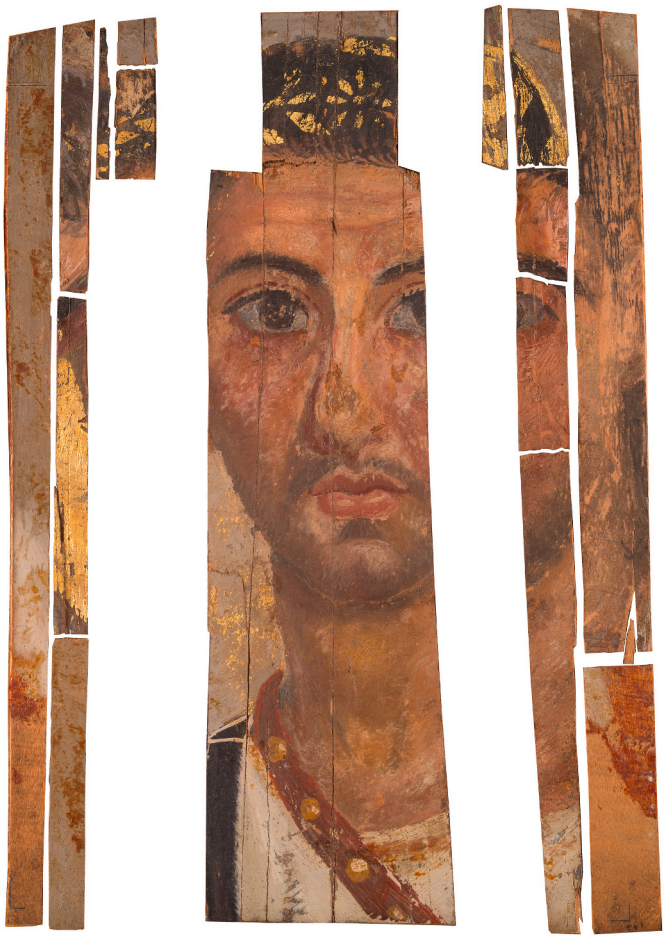

Fig. 13. Digital deconstruction of Composite portrait of a man.

fragments are from other ancient objects, likely other Egyptian funerary portraits. There was little evidence from the analysis that might link the added fragments to one another. However, the lead isotope analysis has suggested a potential workshop connection between the central fragments and a small set of added fragments (6, 12 and 15). Similarities in painting technique, such as the use of a dark gray ground layer, between these three fragments and the central fragments also supports this potential connection.

As part of a collection in a teaching museum, the portrait, aided by the technical investigation, is used to highlight different ways of looking at an artwork, different artistic practices, and differences in collecting policies, opening up the discussion of why an object such as this exists. The portrait remains in its current form, a complicated composite of multiple painted fragments, glued to a board to create the illusion of a single, complete painting. In this form the portrait serves as a reminder of past, destructive practices. However, the power of technology means that the portrait can digitally be deconstructed into its multiple components (Fig. 13) allowing them to be viewed independently.

Overall, this study has provided a better understanding of why this portrait looks the way it does, but perhaps more importantly, this study has identified that multiple individuals are represented in this one portrait and each can now be acknowledged and honored.

Funding

Lead isotope ratio measurements were conducted in the framework of project C14/19/060 funded by the KU Leuven Research Council, while additional support was provided by the Centre for Archaeological Sciences.

Declaration of competing interest

The authors declare that they have no known competing financial interests or personal relationships that could have appeared to influence the work reported in this paper.

Acknowledgements

The authors thank Alicia Van Ham-Meert and Kris Latruwe for performing chemical preparation and lead isotope analysis at KU Leuven and Ghent University, and Richard Newman at the Museum of Fine Arts Boston for his assistance with the SEM-EDX work conducted on the cross-section samples.

Appendix A. Supplementary data

Supplementary data to this article can be found online at https://doi.org/10.1016/j.fsisyn.2023.100442.

References

[1] Ancient Panel Paintings: Examination, Analysis, and Research (APPEAR) project. https://www.getty.edu/projects/appear-project/(accessed 31 January 2023).

[2] Funerary Portraits from Roman Egypt: Facing Forward, August 27, 2022–December 30, 2022, University Research Gallery, Harvard Art Museums, https://harvardartmuseums.org/exhibitions/6194/funerary-portraits-from-roman-egypt-facing-forward (accessed 31 January 2023). See also: https://harvardartmuseums.org/tour/770 (accessed 27 April 2023).

[3] Investigating Herakleides: A Portrait Mummy from Roman Egypt. https://artsandculture.google.com/story/GgVxX_XCuyQUrw (accessed 12 September 2023).

[4] J. Mazurek, M. Svoboda, M. Schilling, GC/MS characterization of beeswax, protein, gum, resin, and oil in romano-Egyptian paintings, Heritage 2 (3) (2019) 1960–1985, https://doi.org/10.3390/heritage2030119.

[5] R. Radpour, G.A. Gates, I. Kakoulli, J.K. Delaney, Identification and mapping of ancient pigments in a Roman Egyptian funerary portrait by application of reflectance and luminescence imaging spectroscopy, Heritage Sci. 10 (2022) 8, https://doi.org/10.1186/s40494-021-00639-5.

[6] A.D. Fovo, M. Fedi, G. Federico, L. Liccioli, S. Barone, R. Fontana, Multi-analytical characterization and radiocarbon dating of a roman Egyptian mummy portrait, Molecules 26 (17) (2021) 5268, https://doi.org/10.3390/molecules26175268.

[7] L. Bradley, J. Ford, D. Kriss, V. Schussler, F. Pozzi, E. Basso, L. Bruno, Evaluating multiband reflectance image subtraction for the characterization of indigo in romano-Egyptian funerary portraits, in: Marie Svoboda, Caroline R. Cartwright (Eds.), Mummy Portraits of Roman Egypt: Emerging Research from the APPEAR Project, J. Paul Getty Museum, Los Angeles, 2020, pp. 68–78. https://www.getty.edu/publications/mummyportraits/part-one/7/.

[8] D.P. Kirby, M. Svoboda, J. Mazurek, L. Rosa Spaabæk, J. Southon, Characterization of an unusual coating on funerary portraits from Roman Egypt circa 100-300AD, Heritage Sci. 11 (2023) 73, https://doi.org/10.1186/s40494-023-00908-5.

[9] J.L. Willams, C.C. Cartwright, M. Walton C, Defining a romano-Egyptian painting workshop at tebtunis, in: M. Svoboda, C.R. Cartwright (Eds.), Mummy Portraits of Roman Egypt: Emerging Research from the APPEAR Project, Getty Publications, Los Angeles, 2020, pp. 132–135. https://www.getty.edu/publications/mummyportraits/part-two/14/.

[10] J. Salvant, J. Williams, M. Ganio, F. Casadio, C. Daher, K. Sutherland, L. Monico, F. Vanmeert, S. De Meyer, K. Janssens, C. Cartwright, M. Walton, A roman eyptian painting workshop: technical investigation of the portraits from tebtunis Egypt, Archeometry 60 (4) (2018) 815–833, https://doi.org/10.1111/arcm.12351.

[11] Portrait of a Woman, Saint Louis art museum Accession no. 128 1951. https://www.slam.org/collection/objects/186/ (accessed 12 September 2023).

[12] Funerary Portraits from Roman Egypt: Facing Forward, Looking for the Saint Louis Painter: Material Composition. https://harvardartmuseums.org/tour/770/slide/12418 (accessed 12 September 2023).

[13] F. Hagen, K. Ryholt, The Antiquities Trade in Egypt 1880-1930: the H. O. Lange Papers, Copenhagen, Det Kongelige Danske Videnskabernes Selskab, 2016.

[14] Guidelines to Collecting and Prevenance. https://harvardartmuseums.org/collections/collecting-policy#provenance (accessed 31 August 2023).

[15] B. Borg, Der zierlichste Anblick der Welt …, Ägyptische Porträtmumien, Philipp von Zabern, Mainz, 1998, pp. 54–55, fig. 68.

[16] Mumienporträt eines jungen Soldaten, Staatliche Museen zu Berlin, Antikensammlung, Ident. Nr.: 31161, vol. 6. https://id.smb.museum/object/681447/mumienportr%C3%A4t-eines-jungen-soldaten (accessed 31 January 2023) and Mumienporträt eines bärtigen Soldaten, Ident. Nr.: 31161,2. https://id.smb.museum/object/681431/mumienportr%C3%A4t-eines-b%C3%A4rtigen-soldaten (accessed 17 April 2023)..

[17] K. Parlasca, Vol 1. of *Repertorio d'arte dell'Egitto: greco-romano Serie B; Ritratti di mummie*, Officine Tipo-Litografiche I.R.E.S., Palermo 35 (1969) 35, pl. 11 fig. 1 and N. 113 pp. 57, pl. 27 fig 3.

[18] B. Borg, Mumienporträts: Chronologie und kultureller Kontext, Philipp von Zabern, Mainz, 1996, pp. 74–75.

[19] D. Barrett Tanner, Four fayum portraits in the Fogg art museum, Bull. Fogg Art Museum 2 (1) (1932) 4–9.

[20] K. Parlasca, Vol. 2 of Repertorio d'arte dell'Egitto greco-romano Serie B: ritratti di mummie, L'Erma di Bretschneider, Rome 353 (56) (1977) pl. 85 fig. 6.

[21] K. Parlasca, Vol. 3 of *Repertorio d'arte dell'Egitto greco-romano Serie B; Ritratti di mummie*, L'Erma di Bretschneider, Rome 567 (40) (1980) pl. 137 fig. 4.

[22] K. Parlasca, H.G. Frenz, Vol. 4 of *Repertorio d'arte dell'Egitto: greco-romano Serie B; Ritratti di mummie*, L'Erma di Bretschneider, Rome 777 (64) (2003) pl. 173, fig. 2 and N 779 pp. 64, pl. 173 fig. 4.

[23] D. Thompson, A lost patchwork "fayum portrait", Am. J. Archaeol. 85 (4) (1981) 491–492, https://doi.org/10.2307/504875.

[24] B. A. Price, B. Pretzel, S. Quillen Lomax, Infrared and Raman Users Group Spectral Database. http://www.irug.org/search-spectral-database/spectra-index (accessed 9 June 2021).

[25] B. Lafuenete, R.T. Downs, Y. Yang, N. Stone, The power of databases: the RRUFF project, in: T. Armbruster, R.M. Danisi (Eds.), Highlights in Mineralogical Crystallography, W. De Gruyter, Berlin, 2015, pp. 1–30. https://rruff.info, 9th June 2021.

[26] C.R. Cartwright, The principles, procedures and pitfalls in identifying archaeological and historical wood samples, Ann. Bot. 116 (1) (2015) 1–13. http://aob.oxfordjournals.org/content/116/1/1.full.pdf+html?sid=4f94de01-bdf1-4496-947bc9d35981f8da.

[27] C.R. Cartwright, Understanding wood choices for ancient panel painting and mummy portraits in the APPEAR project through scanning electron microscopy, in: M. Svoboda, C.R. Cartwright (Eds.), Mummy Portraits of Roman Egypt: Emerging Research from the APPEAR Project, Getty Publications, Los Angeles, 2020, pp. 16–23. www.getty.edu/publications/mummyportraits/part-one/2/.

[28] Center for applied isotope studies at the university of Georgia, radiocarbon dating by AMS. https://cais.uga.edu/service/radiocarbon-dating-by-ams/ (accessed 31 January 2013).

[29] C. Bronk Ramsey, Bayesian analysis of radiocarbon dates, Radiocarbon 51 (1) (2009) 337–360. https://c14.arch.ox.ac.uk/oxcal/OxCal.html (accessed 22 June 2022), doi:10.1017/S0033822200033865.

[30] P. Reimer, W. Austin, E. Bard, A. Bayliss, P. Blackwell, C. Bronk Ramsey, M. Butzin, H. Cheng, R. Edwards, M. Friedrich, P. Grootes, T. Guilderson, I. Hajdas, T. Heaton, A. Hogg, K. Hughen, B. Kromer, S. Manning, R. Muscheler, J. Palmer, C. Pearson, J. van der Plicht, R. Reimer, D. Richards, E. Scott, J. Southon, C. Turney, L. Wacker, F. Adolphi, U. Büntgen, M. Capano, S. Fahrni, A. Fogtmann-Schulz, R. Friedrich, P. Köhler, S. Kudsk, F. Miyake, J. Olsen, F. Reinig, M. Sakamoto, A. Sookdeo, S. Talamo, The IntCal20 Northern Hemisphere radiocarbon age calibration curve (0–55 cal kBP), Radiocarbon 62 (4) (2020) 725–727, https://doi.org/10.1017/RDC.2020.41.

[31] F. Rademaker, G. Verly, C. Somaglino, P. Degryse, Geochemical changes during Eyptian copper smelting? An experimental approach to the Ayn Soukhna process and broader implications for archaeometallurgy, J. Archaeol. Sci. 122 (2020), 105223, https://doi.org/10.1016/j.jas.2020.105223.

[32] Portrait of a man, Harvard Art Museums, Accession No. 1923.59. https://harvardartmuseums.org/collections/object/292324?position=0 (accessed 14 February 2023).

[33] R. Newman, G. Gates, The matter of madder in the ancient world, in: M. Svoboda, C.R. Cartwright (Eds.), Mummy Portraits of Roman Egypt: Emerging Research from the APPEAR Project, Getty Publications, Los Angeles, 2020, pp. 24–33. www.getty.edu/publications/mummyportraits/part-one/3/.

[34] M.V. Orna, M.J.D. Low, N.S. Baer, Synthetic blue pigments: ninth to sixteenth centuries. I. Literature, Stud. Conserv. 25 (1980) 53–63, https://doi.org/10.1179/sic.1980.25.2.53.

[35] J. Riederer, Egyptian blue, in: E.W. Fitzhugh (Ed.), Artists' Pigments. A Handbook of Their History and Characteristics, vol. 3, Archetype, London, 1997, pp. 23–45.

[36] G. Thiboutot, Egyptian blue in romano-Egyptian mummy portraits, in: M. Svoboda, C.R. Cartwright (Eds.), Mummy Portraits of Roman Egypt: Emerging Research from the APPEAR Project, Getty Publications, Los Angeles, 2020, pp. 46–53. https://www.getty.edu/publications/mummyportraits/part-one/5/.

[37] M. Ganio, J. Salvant, J. Williams, L. Lee, O. Cossairt, M. Walton, Investigating the use of Egyptian blue in Roman Egyptian portraits and panels from Tebtunis, Egypt, Appl. Phys. A 121 (2015) 813–821, https://doi.org/10.1007/s00339-015-9424-5.

[38] The APPEAR Project Data. 23 June 2021 Extract, The J. Paul Getty Museum, 2022. https://public.tableau.com/views/APPEARData/APPEARData (accessed 22 August 2023).

[39] Mummy portrait, Phoebe A. Hearst Museum of Anthropology, Accession no. Acc.54/56/63/107. https://portal.hearstmuseum.berkeley.edu/catalog/88445339-1979-446c-b90c-59b3dc2d5efd (accessed 22 August 2023).

[40] S. Knudsen, Cats. 155–156: Two Mummy Portraits, in K. A. Raff, Roman Art at the Art Institute of Chicago, Chicago: Art Institute of Chicago. https://publications.artic.edu/roman/reader/romanart/section/1965/1965 (accessed 26 September 2023)..

[41] E. Mayberger, J. Arista, M. Svoboda, M. Gleeson, Invisible brushstrokes revealed: technical imaging and research of romano-Egyptian mummy portraits, in: M. Svoboda, C.R. Cartwright (Eds.), Mummy Portraits of Roman Egypt: Emerging Research from the APPEAR Project, Getty Publications, Los Angeles, 2020, pp. 79–89. www.getty.edu/publications/mummyportraits/part-one/8/.

[42] C.R. Cartwright, Report on the Wood Identifications of Five Mummy Portraits in the Harvard Art Museums, British Museum Unpublished Report, 2022.

[43] L. Lee, S. Quirke, Painting materials, in: P.T. Nicholson, I. Shaw (Eds.), Ancient Egyptian Materials and Technology, Cambridge University Press, Cambridge, 2000, pp. 104–120.

[44] D.A. Scott, A review of ancient Egyptian pigments and cosmetics, Stud. Conserv. 61 (2000) 185–202, https://doi.org/10.1179/2047058414Y.0000000162.

[45] P. Degryse, J. Schneider, V. Lauwers, M. Waelkens, P. Muchez, Radiogenic isotopes in the provenance determination of raw materials: a case of lead and glass recycling at Sagalassos (SW Turkey), J. Nordic Archeol. Sci. 16 (2009) 15–23.